Design of Low-Pass Filters Using Defected Ground Structure

Jong-Sik Lim, *Member, IEEE*, Chul-Soo Kim, *Member, IEEE*, Dal Ahn, *Senior Member, IEEE*, Yong-Chae Jeong, *Member, IEEE*, and Sangwook Nam, *Member, IEEE*

***Abstract*—A method to design low-pass filters (LPF) having a defected ground structure (DGS) and broadened transmission-line elements is proposed. The previously presented technique for obtaining a three-stage LPF using DGS by Lim *et al.* is generalized to propose a method that can be applied in design N-pole LPFs for $N \leq 5$. As an example, a five-pole LPF having a DGS is designed and measured. Accurate curve-fitting results and the successive design process to determine the required size of the DGS corresponding to the LPF prototype elements are described. The proposed LPF having a DGS, called a DGS-LPF, includes transmission-line elements with very low impedance instead of open stubs in realizing the required shunt capacitance. Therefore, open stubs, tee- or cross-junction elements, and high-impedance line sections are not required for the proposed LPF, while they all have been essential in conventional LPFs. Due to the widely broadened transmission-line elements, the size of the DGS-LPF is compact.**

***Index Terms*—Defected ground structure (DGS), low-pass filters (LPFs), periodic structures.**

I. Introduction

IT IS well known that typical properties of low-pass filters (LPFs) can be obtained by adding periodic structures to transmission lines. The representative periodic structures for planar transmission lines and/or microwave circuits are photonic bandgap (PBG) and defected ground structure (DGS) [2]–[5]. The PBG has been known as a popular periodic structure for planar transmission lines. However, drawbacks of PBGs have been also discussed as follows.

1) A large area is needed because a number of periodic patterns should be adopted.
2) It is obscure to define the unit element, and difficult to extract the equivalent-circuit elements for the PBG unit element.
3) Therefore, it is very restricted to extend its practical application to microwave circuits. To the contrary, one can easily define the unit element of the DGS and model the equivalent circuit.

Manuscript received July 15, 2004; revised February 14, 2005. This work was supported by the RRC Program through the Soonchunhyang University Wireless Components Research Center.

J.-S. Lim and D. Ahn are with the Division of Information Technology Engineering, Soonchunhyang University, Asan, Chungnam 336-745, Korea (e-mail: jslim@sch.ac.kr).

C.-S. Kim is with the Samsung Advanced Institute of Technology, Yongin 449-712, Korea.

Y.- C. Jeong is with the Division of Electronics and Information Engineering, Chonbuk National University, Jeonju 561-756, Korea.

S. Nam is with the School of Electrical Engineering and Computer Science, Seoul National University, Seoul 151-742, Korea.

Digital Object Identifier 10.1109/TMTT.2005.852765

In addition, since only a few DGS elements show the typical properties of periodic structures, the resultant circuit size becomes relatively small. Furthermore, the structure of the DGS is simple and it is easy to design the DGS pattern. For these reasons, since [4] has introduced the structure and called it a DGS for the first time, the DGS has been extensively applied to design microwave circuits such as filters, power dividers, couplers, amplifiers, oscillators, and so on [1], [6]–[12].

There is much previous research about the characteristics of LPFs having periodic structures on microstrip or coplanar waveguide (CPW) transmission lines [13]–[16]. However most of them are not analytical because they mainly depend on electromagnetic (EM) simulations to design LPFs and predict circuit performances. To the contrary, in the design of LPFs using DGSs including this study, all design steps are based on theories and reasonable explanations as follows.

- The equivalent-circuit elements of the DGS is extracted and used for replacing the series inductances in the LPF prototype circuit.
- The LPF is composed of the extracted equivalent lumped elements, thus, it is an ideal LPF, is designed, and is compared to the realized LPF using the DGS practically.

Two methods to design a three-pole LPF using the DGS has been proposed in [1] and [6]. In these papers, the sizes of two DGS patterns in the LPF were exactly the same because two inductances in the three-pole "L_1 (series)- C_2 (shunt)- L_3 (series)" prototype LPF are identical. In [6], discontinuity elements such as tee- or cross-junctions were adopted to connect open stubs to realize the shunt capacitance. However, in the three-pole LPF proposed in [1], there are no junction elements, thin transmission lines for high impedance, or open stubs. In addition, the width of the transmission-line elements in the LPF has been remarkably broadened. Thus, advantages such as compact design and error-robust realization in fabricating the layout have been obtained.

However, in order to design N-stage ($N \geq 5$) LPFs using the DGS, e.g., a five-stage like "L_1 (series)-C_2 (shunt)-L_3 (series)-C_4 (shunt)-L_5 (series)," two different dimensions of the DGS have to be adopted because L_3 is not equal to L_1, although $L_1 = L_5$. In order to select the proper dimension of the DGS for L_3, careful consideration based on filter theories, extracted equivalent-circuit elements of various DGS dimensions, and some related topics of transmission lines should be taken. The size of the DGS for L_3 is determined by accurate curve-fitting results for equivalent-circuit elements to correspond exactly to the required inductance. In addition, the length of transmission-line elements between DGS patterns is determined through the consideration for the equivalent capacitance and additional para-

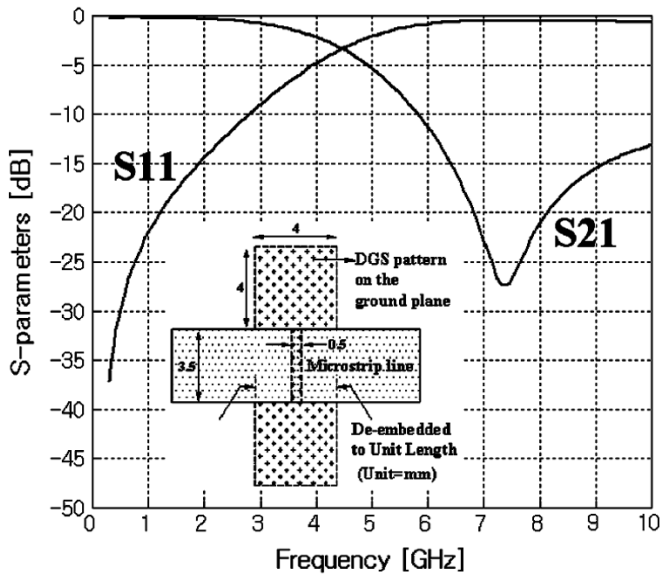

Fig. 1. Microstrip line with a dumb-bell-shaped DGS pattern and S-parameters by an EM simulation ($\varepsilon_r = 3.48$, substrate thickness $= 30$ mil).

sitic inductance, as well as the required shunt capacitances in the prototype LPF. Therefore, a design of a five-pole DGS-LPF requires many more complex steps than the previous three-pole DGS-LPF shown in [1] and [6].

Thus, the goal of this paper is to propose a new technique to design an N-pole LPF having ("DGS-LPF"), and to generalize the previous design method for $N \geq 5$ using different sizes of DGS patterns. For this purpose, modeling for the equivalent circuit of the DGS, a curve fitting for determining the required different sizes of the DGS that reflects the inductance values in the prototype LPF and a practical design example will be successively discussed.

In order to show the validity of the proposed method, a five-pole DGS-LPF, as an example, is designed and measured in this paper. The proposed five-pole DGS-LPF has a much wider microstrip line than conventional microstrip LPFs, and does not include high-impedance lines, which have been essentially required in conventional design. The series inductances in the prototype LPF are realized by DGSs, while the shunt capacitances are realized by the widely compensated transmission line. Therefore, no discontinuity elements such as tee- or cross-junction for connecting open stubs are required because there are no open stubs in the proposed DGS-LPF.

II. DGS Pattern and Modeling for the Equivalent Circuit

Fig. 1 shows a microstrip line having a dumb-bell-shaped DGS and its S-parameters from an EM simulation. Two rectangular defected areas and one connecting slot correspond to the equivalently added inductance (L) and capacitance (C), respectively. Accordingly, a resonance occurs at a certain frequency because of the parallel L–C circuit. Inversely, it is intuitively known that the equivalent circuit includes a pair of parallel inductor–capacitor from the resonant phenomenon in the S-parameter. This means the microstrip line having the DGS does not have all-pass characteristics, but restricted passband properties. In addition, slow-wave characteristics are observed due to the added L–C components of the DGS [3], [5], [9]. The defected areas can be realized by not only rectangle, but also other geometries such as triangle, circle, hexagon, octagon, spiral, and so on. For convenience, squares are used in Fig. 1.

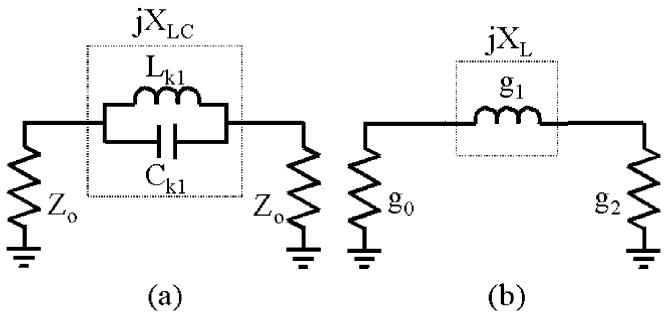

Fig. 2. (a) Equivalent circuit of the microstrip line with unit DGS. (b) Butterworth prototype of one-pole LPF.

It is very clear that the resonant frequency (ω_o) of the DGS and 3-dB cutoff frequency $(\omega_{c,3\,\mathrm{dB}})$ exist as shown in Fig. 1. The equivalent L–C circuit of the DGS can be extracted because this kind of electrical characteristic is observed from a typical L–C parallel resonant circuit.

The equivalent circuit of the DGS and one-pole Butterworth prototype of the LPF are presented the DGS in Fig. 2. The equivalent L–C elements are calculated by (1)–(3) because two reactance values of Fig. 2(a) and (b) must be equal at $\omega_{c,3\,\mathrm{dB}}$ as follows:

$$X_{LC} = \frac{1}{\omega_o C_{k1}\left(\dfrac{\omega_o}{\omega} - \dfrac{\omega}{\omega_o}\right)} \tag{1}$$

$$X_L = \omega' Z_o g_1 \tag{2}$$

$$X_{LC}|_{\omega=\omega_{c,3\,\mathrm{dB}}} = X_L|_{\omega'=1} \tag{3}$$

where $\omega'(=1), g_1(=2)$, and $Z_o(=50\ \Omega)$ are the normalized 3-dB cutoff frequency, element value of one-pole Butterworth prototype LPF, and port impedance, respectively, and $\omega_o = (1/\sqrt{L_{k1}C_{k1}})$. The calculated L_{k1} and C_{k1} of the DGS shown in Fig. 1 are 2.2832 nH and 0.2026 pF, respectively. Fig. 3 shows an excellent agreement between the previous S-parameters shown in Fig. 1 and the new ones calculated using L_{k1} and C_{k1}. Advanced Design System (ADS), a circuit simulator from Agilent Technologies, has been used for the calculation. This agreement means that the modeling technique is valid in extracting the equivalent-circuit elements. It should be noted that this is one of the great advantages of DGS because it is possible to define the unit element of the DGS and to establish the equivalent circuit of it, while the conventional planar transmission lines with a periodic structure such as a PBG have difficulty in defining the unit element and to extract the modeled circuit element.

III. Design of Five-Pole LPF Using DGS

A. Prototype LPF and Adoption of DGS

The method to design a five-pole LPF using the DGS is discussed here. Fig. 4 depicts the prototype circuit of a five-pole

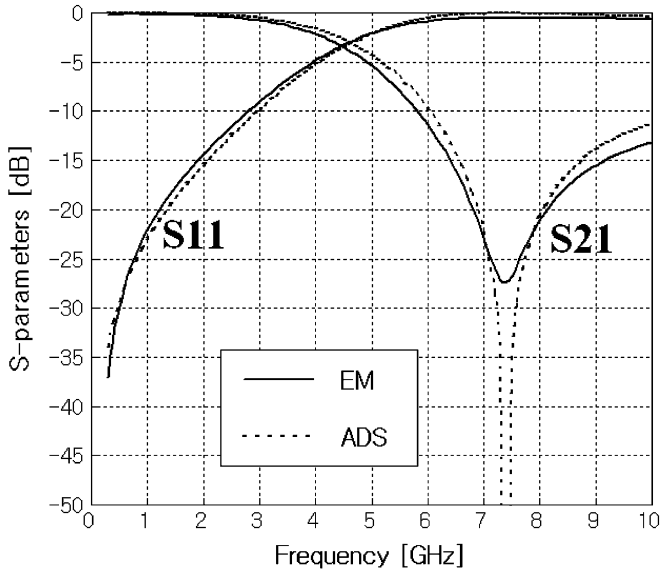

Fig. 3. S-parameters of the equivalent L_{k1}-C_{k1} network with the EM simulation results overlapped.

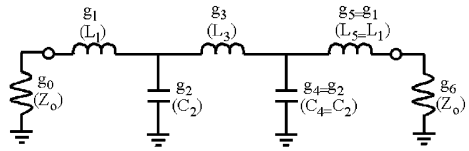

Fig. 4. Five-pole Chebyshev prototype LPF.

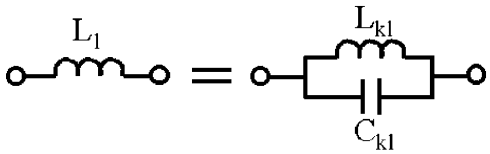

Fig. 5. Equality of a series inductor to an L–C parallel circuit.

LPF. Here, $g_i (i = 0, 1, 2, 3, 4, 5, 6)$ represent the normalized element values of a Chebyshev prototype LPF for the given ripple [17]. According to the design theory of filters, in order to transform the prototype LPF to the LPF composed of lumped elements, the values of L_1, C_2, L_3, C_4, and L_5 can be determined owing to the impedance and frequency scaling rules expressed in (4)–(6). Here, ω_c means the cutoff frequency of the LPF

$$L_1 = \frac{g_1 Z_o}{\omega_c} = \frac{g_5 Z_o}{\omega_c} = L_5 \tag{4}$$

$$L_3 = \frac{g_3 Z_o}{\omega_c} \tag{5}$$

$$C_2 = \frac{g_2}{Z_o \omega_c} = \frac{g_4}{Z_o \omega_c} = C_4. \tag{6}$$

In order to replace L_1 by the DGS shown in Fig. 1, the equivalence illustrated in Fig. 5 should be satisfied at ω_c; hence, two reactance values must be equal, as expressed in (7). The cutoff frequency (ω_c) of the LPF to be designed is determined by equating (4) and (7). The resultant ω_c is expressed as (8). Finally, since the equivalent L_{k1} and C_{k1} of the DGS in Fig. 1 are 2.2832 nH and 0.2026 pF, ω_c is 2.366 GHz. Now the values of L_1, C_2, L_3, C_4, and L_5 can be calculated after having been

TABLE I
PROTOTYPE ELEMENTS OF THE FIVE-POLE CHEBYSHEV LPF WITH 0.01-dB RIPPLE AND TRANSFORMED ELEMENTS

Prototype elements	Element values	Scaled elements	Scaled element values	Final elements	Final element values
g_0	1	Z_o (Ω)	50		
g_1	0.7563	L_1 (nH)	2.5433	L_{k1}-C_{k1} (nH-pF)	2.2832 - 0.2026
g_2	1.3049	C_2 (pF)	1.7552	C_{k2} (pF)	1.7552
g_3	1.5773	L_3 (nH)	5.3041	L_{k3}-C_{k3} (nH-pF)	4.2862 - 0.2026
g_4	1.3049	$C_4 = C_2$ (pF)	1.7552	C_{k2} (pF)	1.7552
g_5	0.7563	$L_5 = L_1$ (nH)	2.5433	L_{k1}-C_{k1} (nH-pF)	2.2832 - 0.2026
g_6	1	Z_o (Ω)	50		

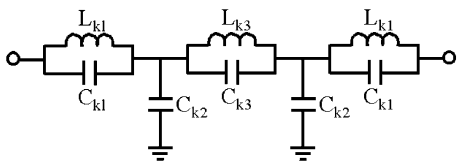

Fig. 6. Modified five-pole prototype LPF using an L–C resonator.

transformed by frequency and impedance scaling. The resultant L_1, C_2, L_3, C_4, and L_5 for the five-pole Chebyshev with a 0.01-dB ripple are summarized in Table I as follows:

$$\frac{1}{\omega_c L_1} = -\left(\omega_c C_{k1} - \frac{1}{\omega_c L_{k1}}\right) \tag{7}$$

$$\omega_c = -\frac{L_{k1}\omega_o^2}{2 g_1 Z_o} + \sqrt{\frac{\omega_o^4}{4}\left(\frac{L_{k1}}{g_1 Z_o}\right)^2 + \omega_o^2}. \tag{8}$$

Fig. 6 shows the new prototype five-pole LPF of which three inductors have been replaced by the L–C parallel equivalent circuit of the DGS. Since L_5 is equal to L_1, the parallel resonator of L_{k5}–C_{k5} is exactly same as the L_{k1}–C_{k1} resonator. In additional, the shunt capacitors C_2 and C_4 are also exactly the same, and are expressed as C_{k2} in Fig. 6.

B. Determination of the DGS for L_3

It should be noted that the size of the new DGS for L_3 is different from the DGS shown in Fig. 1 because L_3 is not equal to L_1. Equation (9) represents the equivalence of L_3 and the new DGS for L_{k3}–C_{k3} at ω_c. Since ω_c and L_3 are known already above, the next step is to determine the dimension of the DGS for L_3 (DGS3)

$$\frac{1}{\omega_c L_3} = -\left(\omega_c C_{k3} - \frac{1}{\omega_c L_{k3}}\right). \tag{9}$$

The equivalent inductance (L) and capacitance (C) of the DGS are originated mainly from the outer length of rectangular defected area and connecting slot, respectively. According to

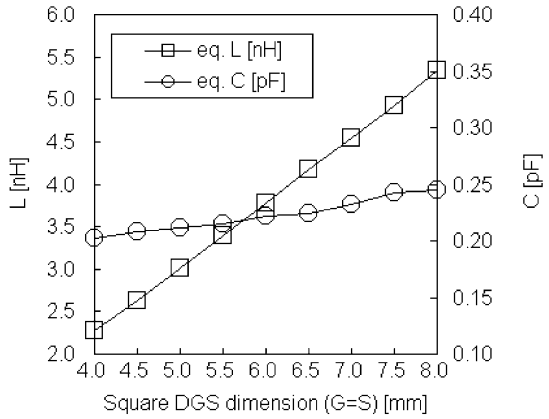

Fig. 7. Equivalent L–C values versus the dimension of the DGS for the fixed size of the connecting slot (0.5 mm × 3.5 mm)

Fig. 7, the equivalent L and C depend on the dimensions of the defected area when the size of connecting slot is fixed to be 0.5 mm × 3.5 mm, as shown in Fig. 1. The equivalent L is proportional to the dimension of the defected area directly, while the equivalent C is nearly constant.

It is a reasonable approximation that C_{k3} is almost equal to C_{k1} irrespective of the dimension of defected area because the equivalent capacitance is almost constant under the fixed dimensions of connecting slot. If the connecting slot of the DGS3 is fixed to be the same dimensions for convenience, i.e., 0.5 mm × 3.5 mm, C_{k3} becomes known and L_{k3} becomes unknown. Finally, L_{k3} is calculated to be 4.2862 nH by (10) as follows:

$$L_{k3} = \frac{1}{\frac{1}{L_3} + \omega_c^2 C_{k3}}. \tag{10}$$

The required size of the DGS3 for L_{k3} can be found effectively through the curve fitting shown in Fig. 8. The trends of equivalent L and C versus dimensions of the DGS under the fixed connecting slot (0.5 mm × 3.5 mm) are plotted in Fig. 8 with the fitted results overlapped. The fitted equivalent L and C are very exact, and the percentage errors of the curve fitting for the equivalent L and C are only 0.1% and 0.25%, respectively. Fig. 8 plays a great role in determining the size of the DGS3, which reflects the required L_{k3} to design LPFs. Now the size of the DGS3 can be determined in this case. The dimension of $G\ (=\ S)$ for $L_{k3}\ (=\ 4.2862$ nH) is found to be 6.66 mm from Fig. 8 or the established equation for fitting. In addition, the equivalent capacitance C_{k3} is 0.228 pF when $G = S = 6.66$ mm.

It should be noted that C_{k3} has been approximated to be the same as $C_{k1}\ (= 0.2026$ pF), but here, C_{k3} is 0.228 pF. Although the difference ($0.228\,pF - 0.2026\,pF = 0.0254$pF) is so small that it can be ignored, it is possible to compensate it by slightly tuning the dimension of the DGS3. In order for the reactance (jX_{LC}) of the DGS3 to be unchanged, L_{k3} should be tuned to be 4.1855 nH. The equality between two reactances is satisfied at $\omega_c; jX_{4.2862\text{ nH}-0.2026\text{ pF}} = jX_{4.1855\text{ nH}-0.228\text{ pF}}$. The size of the DGS for 4.1855 nH is 6.55 mm in Fig. 8(a). When G is 6.55 mm, the equivalent capacitance is 0.227 pF from

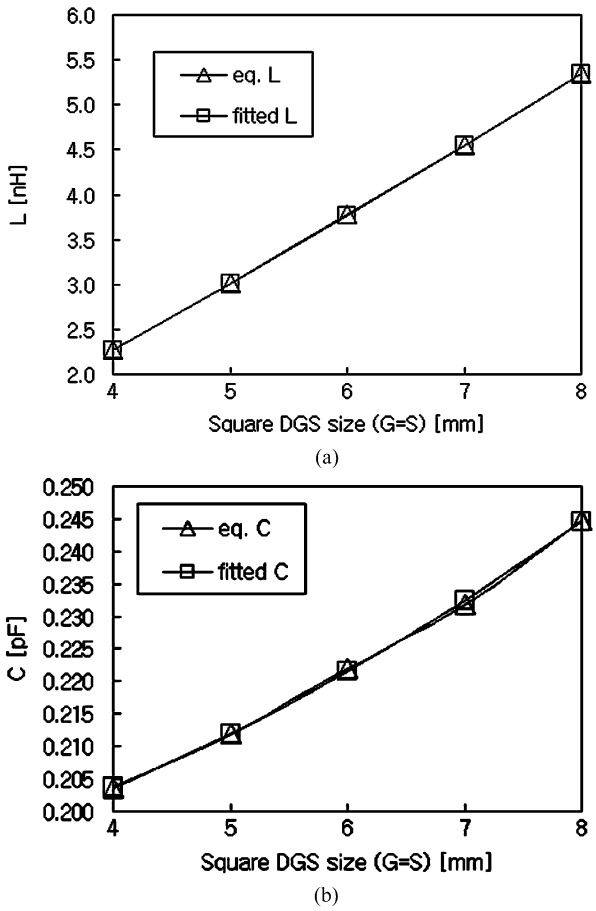

Fig. 8. (a) Equivalent L and C curve-fitted L values. (b) Equivalent C and curve-fitted C values versus the dimension $(G = S)$ of the DGS for the fixed connecting slot (0.5 mm × 3.5 mm)

Fig. 8(b). It should be noted that the equivalent capacitance is being kept to be almost constant (0.228 pF → 0.227 pF), while G has been reduced to 6.55 mm. This is a reasonable result because the size of the DGS has changed slightly (6.66 mm → 6.55 mm) with the fixed connecting slot. This is another proof that the equivalent capacitance of the DGS is produced by the connecting slot.

The predicted layout of the proposed five-pole DGS-LPF, which is based on the described steps thus far, is illustrated in Fig. 9. However, since the broad microstrip lines between DGS patterns, which are required for replacing the shunt capacitances $C_{k2}(=C_{k4})$, have an additional small equivalent inductance, the final dimension of the DGS3 should again be reduced to reflect it. This will be discussed in Section III-C in detail.

C. Realization of the Shunt Capacitance C_{k2}

There are three DGS patterns for three series inductors in the prototype five-pole LPF in Fig. 9. Two shunt capacitors in the prototype LPF will be realized by the proper length (D) of the broad microstrip line between DGS patterns. Meanwhile, the size of the DGS3 will be adjusted slightly again because of the additional equivalent inductance of the microstrip line. $G3(=S3)$ in Fig. 9 denotes the dimension of the defected area of the DGS3.

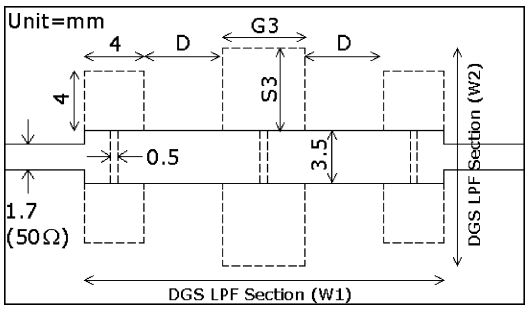

Fig. 9. Layout of the proposed five-pole LPF. Proper D and final $G3(=S3)$ should be determined through further steps to complete the design.

It is necessary to compensate the width of the microstrip line between DGS patterns in order to get the proper capacitive element, and to remove open stubs and junction elements such as tee or cross. This is one of the important features of the proposed DGS-LPF. For this purpose, the width of the broad microstrip line has been fixed by 3.5 mm from the beginning of the design, as shown in Figs. 1 and 9, while the width of the 50-Ω microstrip line is only 1.7 mm. According to the basic theories of transmission lines, a transmission line with low characteristic impedance has a capacitive element equivalently [18]. Hence, the right "D" would results in the required capacitive element, which replaces the shunt capacitor in the prototype LPF, and completes the LPF design.

The equivalent capacitance of a transmission line with the characteristic impedance (Z_o) and length (l) is expressed as (11). However, additional equivalent inductance of the transmission line does also exist at the same time, and it is expressed as L_a in (12). The length (l), corresponding to 1.7552 pF at 2.366 GHz, of the microstrip line with the width of 3.5 mm is 10.6 mm. The produced equivalent inductance (L_a) of a 10.6-mm microstrip line is 0.78 nH. Here, l is the distance between the centers of two neighboring DGS patterns.

Now the final size of the DGS3 can be determined. Since L_3 should include two L_a at both sides, (13) is obtained from (9) and (10). As a result of the consideration for L_a, the inductance, which should be the provided DGS3, is 3.7441 nH, eventually by calculating $L_3' = L_3 - 2L_a$ $(= 5.3041\text{ nH} - 2 \times 0.78\text{ nH})$. Thus, the final L_{k3} is 3.2066 nH from (13) because L_3' is 3.7441 nH, and the corresponding dimension $(G_3 = S_3)$ for the defected square of the DGS3 is 5.25 mm. Finally, D becomes 5.35 mm by calculating "$D = l - G_3 = 10.6\text{ mm} - 5.25\text{ mm}$" as follows:

$$C = \frac{1}{\omega Z_o}\sin\left(\frac{2\pi\ell}{\lambda_g}\right) \tag{11}$$

$$L_a = \frac{Z_o}{2\omega}\sin\left(\frac{2\pi\ell}{\lambda_g}\right) \tag{12}$$

$$L_{k3} \approx \frac{1}{\dfrac{1}{(L_3 - 2L_a)} + \omega_c^2 C_{k3}} = \frac{1}{\dfrac{1}{L_3'} + \omega_c^2 C_{k3}}. \tag{13}$$

Fig. 10 shows the fabricated five-pole DGS-LPF. The upper pattern is simply composed of three transmission-line elements, two of them are 50-Ω microstrip lines for connection. As has been described above, there is no open-stub junction element to connect the open stub, high-impedance line, and the step junctions between very low- and high-impedance lines in the layout of the proposed DGS-LPF. On the contrary, a much broadened microstrip has been selected from the initial stage of design. This guarantees the LPF with a great robustness to manufacturing errors and compact size.

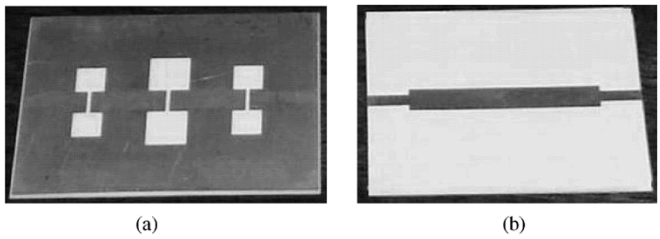

Fig. 10. Five-pole DGS-LPF. (a) Bottom side. (b) Top side.

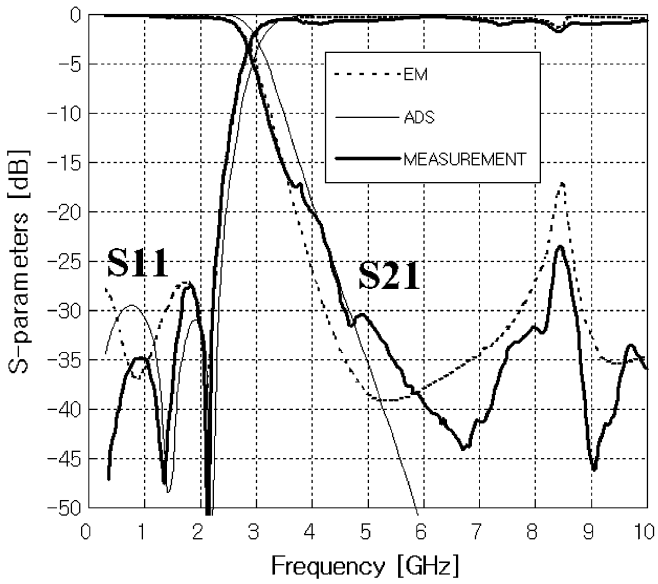

Fig. 11. Performances of the five-pole DGS-LPF.

One may give a question about backside radiation through the defected area. This is a common problem to all circuits having ground-modified structures currently. A good solution is to put the circuit in a metallic housing having bottom holes with a proper depth and shape under the DGS patterns. The rule-of-thumb for depth is at least around five times the substrate thickness.

IV. Performance of the Proposed Five-Pole DGS-LPF

Now the measured S-parameters, the ideal performances of the proposed DGS-LPF, and the comparison between them are discussed. The five-pole DGS-LPF shown in Fig. 10 has been build and measured. Fig. 11 includes three S-parameters, which are: 1) the S-parameters calculated on Agilent ADS for the five-pole LPF, which has the transformed inductances and capacitances in Table I; 2) the S-parameters predicted by Ensemble, an EM simulator from Ansoft, for the layout in Figs. 10; and 3) the measured S-parameters of the fabricated DGS-LPF. Even though some minor disagreements are observed, a great agreement is presented between three S-parameter sets in Fig. 11.

The three reflection coefficients are less than -25 dB and the skirt slopes agree well with each other. It is noted that a local peak occurs at 8.4 GHz in the $S21$ curves from EM simulation and measurement, while it is not seen in the $S21$ plot of the ideal LPF. It is natural result because the ideal LPF composed of only the lumped elements such as series inductances and shunt capacitors has no distributed effects. It is understood that the local peak is due to the fact that the length of the transmission line between DGS patterns is effectively a half-wavelength at 8.4 GHz. However, the local peak is not meaningful any more because $S21$ at 8.4 GHz is around -20 dB without any effective bandwidth. Preferably it can be said that the validity of the proposed design method has been proven evidently via Fig. 11.

In particular, the reflection and rejection-slope characteristics of the proposed DGS-LPF are excellent even though it only has five poles. In the conventional design, much higher N-poles are required to get such a level of skirt slope. However, in the conventional design, it is true that the higher N, the higher the loss and the larger the size. Fig. 11 shows another important feature of the proposed DGS-LPF; harmonic rejection is being obtained over a very wide frequency range although the microstrip line is a distributed element.

V. Conclusion

A new N-pole LPF design method using the DGS has been proposed. The proposed DGS-LPF neither has open stubs, nor high-impedance lines because a very wide microstrip line has been adopted to realize the shunt capacitors. In order to extend the existing design method of the three-pole DGS-LPF to an N-pole DGS-LPF ($N \geq 5$) using different sizes of DGSs, a five-pole DGS-LPF has been design as an example. The method to calculate the cutoff frequency of the LPF has been developed based on the modeled equivalent inductance and capacitance, which depends on the dimension of the DGS pattern. In addition, the method to determine the size of the DGS pattern, which exactly realizes the required transformed inductance, has been proposed by curve fitting with excellent accuracy. Furthermore, the equivalent inductance and capacitance of the microstrip line have been considered to adjust the size of the DGS pattern to get an exact dimension of the DGS.

Open stubs, junction elements, very high-impedance lines, and abrupt step junctions, which have always been adopted in conventional LPFs, are not required in the proposed DGS-LPF. The proposed DGS-LPF has only largely broadened microstrip lines and DGS patterns on the ground plane. It is expected that the broadened width of microstrip line would provide an improved high power-handling capability.

The validity of the proposed design method of the DGS-LPF design has been verified by comparing the three S-parameter sets of the five-pole LPF, i.e.: 1) the S-parameters obtained from circuit simulation for the LPF composed of only ideal lumped inductors and capacitors; 2) the S-parameters calculated on an EM simulator for the final layout of the proposed LPF; and 3) the measured S-parameters. The measured S-parameters are in excellent agreement with the calculated ones, especially in the reflection coefficient, insertion loss in the passband, radical skirt slope, wide rejection band, and so on.

It is anticipated that the proposed design method can be applicable for arbitrary N-stage LPFs, as well as five-stage LPFs. In addition, it is believed that the LPFs composed of CPW transmission lines and DGS patterns can also be designed by applying the proposed design technique and further study.

References

[1] J. S. Lim, C. S. Kim, Y. T. Lee, D. Ahn, and S. Nam, "A new type of low pass filter with defected ground structure," in *Proc. 32nd Eur. Microwave Conf.*, Sep. 2002, pp. 32–36.

[2] V. Radisic, Y. Qian, R. Coccioli, and T. Itoh, "Novel 2-D photonic bandgap structure for microstrip lines," *IEEE Microw. Guided Wave Lett.*, vol. 8, no. 2, pp. 69–71, Feb. 1998.

[3] F. R. Yang, K. P. Ma, Y. Qian, and T. Itoh, "A uniplanar compact photonic-bandgap (UC-PBG) structure and its applications for microwave circuits," *IEEE Trans. Microw. Theory Tech.*, vol. 47, no. 8, pp. 1509–1514, Aug. 1999.

[4] C. S. Kim, J. S. Park, D. Ahn, and J. B. Lim, "A novel 1-D periodic defected ground structure for planar circuits," *IEEE Microw. Guided Wave Lett.*, vol. 10, no. 4, pp. 131–133, Apr. 2000.

[5] T. Y. Yun and K. Chang, "Uniplanar one-dimensional photonic-bandgap structures and resonators," *IEEE Trans. Microw. Theory Tech.*, vol. 49, no. 3, pp. 549–553, Mar. 2001.

[6] D. Ahn, J. S. Park, C. S. Kim, J. Kim, Y. Qian, and T. Itoh, "A design of the low-pass filter using the novel microstrip defected ground structure," *IEEE Trans. Microw. Theory Tech.*, vol. 49, no. 1, pp. 86–93, Jan. 2001.

[7] J. S. Lim, C. S. Kim, J. S. Park, D. Ahn, and S. Nam, "Design of 10 dB 90° branch line coupler using microstrip line with defected ground structure," *Electron. Lett.*, vol. 36, no. 21, pp. 1784–1785, Oct. 2000.

[8] J. S. Lim, S. W. Lee, C. S. Kim, J. S. Park, D. Ahn, and S. Nam, "A 4 : 1 unequal Wilkinson power divider," *IEEE Microw. Wireless Compon. Lett.*, vol. 11, no. 3, pp. 124–126, Mar. 2001.

[9] J. S. Lim, J. S. Park, Y. T. Lee, D. Ahn, and S. Nam, "Application of defected ground structure in reducing the size of amplifiers," *IEEE Microw. Wireless Compon. Lett.*, vol. 12, no. 7, pp. 261–263, Jul. 2002.

[10] Y. T. Lee, J. S. Lim, J. S. Park, D. Ahn, and S. Nam, "A novel phase noise reduction technique in oscillators using defected ground structure," *IEEE Microw. Wireless Compon. Lett.*, vol. 12, no. 2, pp. 39–41, Feb. 2002.

[11] J. S. Lim, C. S. Kim, Y. T. Lee, D. Ahn, and S. Nam, "A spiral-shaped defected ground structure for coplanar waveguide," *IEEE Microw. Guided Wave Lett.*, vol. 12, no. 9, pp. 330–332, Sep. 2002.

[12] Y. T. Lee, J. S. Lim, S. Kim, J. Lee, S. Nam, K. S. Seo, and D. Ahn, "Application of CPW based spiral-shaped defected ground structure to the reduction of phase noise in V-band MMIC oscillator," *IEEE MTT-S Int. Microwave Symp. Dig.*, vol. 3, pp. 2253–2256, Jun. 2003.

[13] F. Martin, F. Falcone, J. Bonache, T. Lopetegi, M. Laso, and M. Sorolla, "Dual electromagnetic bandgap CPW structures for filter applications," *IEEE Microw. Wireless Compon. Lett.*, vol. 13, no. 9, pp. 393–395, May 2001.

[14] I. Rumsey, M. Piket-May, and P. Kelly, "Photonic bandgap structures used as filters in microstrip circuits," *IEEE Microw. Guided Wave Lett*, vol. 8, no. 10, pp. 336–338, Oct. 1998.

[15] Y. Qian, F. Yang, and T. Itoh, "Characteristics of microstrip lines in a uniplanar compact PBG ground plane," in *Proc. Asia–Pacific Microwave Conf.*, Dec. 1998, pp. 589–592.

[16] T. Kim and C. Seo, "A novel photonic bandgap structure for low-pass filter of wide stopband," *IEEE Microw. Guided Wave Lett.*, vol. 10, no. 1, pp. 13–15, Jan. 2000.

[17] G. L. Matthaei, L. Young, and E. M. T. Jones, *Microwave Filters, Impedance-Matching Networks, and Coupling Structures*. Dedham, MA: Artech House, 1980.

[18] A. Sweet, *MIC & MMIC Amplifier and Oscillator Circuit Design*. Boston, MA: Artech House, 1990.

Jong-Sik Lim (S'91–M'94) received the B.S. and M.S. degrees in electronic engineering from Sogang University, Seoul, Korea, in 1991 and 1993, and the Ph.D. degree from the School of Electrical Engineering and Computer Science, Seoul National University, Seoul, Korea, in 2003.

In 1993, he joined the Electronics and Telecommunications Research Institute (ETRI), Daejeon, Korea, where he remained for six years with the Satellite Communications Division as a Senior Member of Research Staff. He was one of the key members in the development of monolithic microwave integrated circuit (MMIC) low-noise amplifiers (LNAs) and solid-state power amplifiers (SSPAs) for the 20/30-GHz satellite transponder at ETRI. From March to July in 2003, he was with the Division of Information Technology, Seoul National University, where he was involved with the Brain Korea 21 Project as a Post-Doctoral Fellow, and gave lectures in the Graduate Schools of Soonchunhyang and Soongsil universities. From July 2003 to September 2004, he was a Patent Examiner with the Korean Intellectual Property Office (KIPO). In September 2004, he rejoined ETRI, where he was involved with the Antenna Technology Research Team as a Senior Research Member. Since March 2005, he has been a faculty member with the Division of Information Technology Engineering, Soonchunhyang University, Asan, Chungnam, Korea. His current research interests include design of the passive and active circuits for RF/microwave and millimeter-wave with microwave integrated circuit (MIC)/MMIC technology, modeling of active device, design of high-power amplifiers for mobile communications, applications of periodic structures to the RF/microwave circuits, and modeling of passive structures having periodic structures.

Dr. Lim is a member of the Institute of Electrical, Information and Communication Engineers (IEICE), Japan, and the Korea Electromagnetic Engineering Society (KEES).

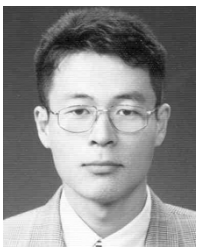

Chul-Soo Kim (S'99–M'02) received the B.S., M.S., and Ph.D. degrees from Soonchunhyang University, Asan, Chungnam, Korea, in 1996, 1998, and 2002, respectively, all in electronics.

From 1991 to 1993, he was with Electronics and Telecommunications Research Institute (ETRI), Daejeon, Korea. Since 1993, he has been with the RF and Microwave Component Research Center (RAMREC) and the BIT Wireless Communication Devices Research Center, Soonchunhyang University. He is currently with the Samsung Advanced Institute of Technology, Yongin, Korea. His current research interests include passive components for wireless communications, DGS circuit applications, and circuit modeling.

Dr. Kim is a member of the Korea Electromagnetic Engineering Society (KEES).

Dal Ahn (M'93–SM'04) received the B.S., M.S., and Ph.D. degrees from Sogang University, Seoul, Korea, in 1984, 1986, and 1990, respectively, all in electronics.

From 1990 to 1992, he was with the Mobile Communications Division, Electronics and Telecommunications Research Institute (ETRI), Daejeon, Korea. Since 1992, he has been with the School of Electrical and Electronic Engineering, Soonchunhyang University, Asan, Chungnam, Korea, where he is currently a Professor. He is also currently Chief of the RF and Microwave Component Research Center (RAMREC), Soonchunhyang University. He is also a Technical Consultant for Tel Wave Inc., Suwon, Korea. His current research interests include the design and application of passive and active components at radio and microwave frequencies, design of the RF front-end module for various handset system using low-temperature co-fired ceramic (LTCC) technology, DGS circuit applications, and circuit modeling using a commercial EM analysis program. He is an Editor of the *Journal of Korea Electromagnetic Engineering Society*.

Prof. Ahn is a senior member of the Korea Electromagnetic Engineering Society (KEES).

Yong-Chae Jeong (M'93) received the B.S., M.S., and Ph.D. degrees from Sogang University, Seoul, Korea, in 1989, 1991, and 1996, respectively all in electronics.

From 1991 to 1998, he was a Senior Engineer with Samsung Electronics. In 1998, he joined the Division of Electronics and Information Engineering and the Institute of Information and Communication, Chonbuk National University, Chonju, Korea. He is currently an Associate Professor and teaches and conducts research in the area of microwave devices, base-station amplifiers, and linearizing technology.

Prof. Jeong is a member of the Korea Electromagnetic Engineering Society (KEES).

Sangwook Nam (S'87–M'88) received the B.S. degree from Seoul National University, Seoul, Korea, in 1981, the M.S. degree from the Korea Advanced Institute of Science and Technology, Seoul, Korea, in 1983, and the Ph.D. degree from the University of Texas at Austin, in 1989, all in electrical engineering.

From 1983 to 1986, he was a Researcher with the Gold Star Central Research Laboratory, Seoul, Korea. Since 1990, he has been with Seoul National University, where he is currently a professor with the School of Electrical Engineering and Computer Science. His research interests include analysis/design of EM structures, antennas, and microwave active/passive circuit. He is an Editor of the *Journal of Korea Electromagnetic Engineering Society*.

Prof. Nam is a member of the Korea Electromagnetic Engineering Society (KEES).